31st EPS Conference on Plasma Phys. London, 28 June - 2 July 2004 ECA Vol.**28G**, P-4.141 (2004)

# Impurity Transport in 3D Plasma Edge Turbulence

V. Naulin, O.E. Garcia, A.H. Nielsen, J. Juul Rasmussen and H. Bindslev
Association EURATOM – Risø National Laboratory
Optics and Plasma Research, OPL-128 Risø, 4000 Roskilde, Denmark

We investigate the transport of impurities in drift-Alfvén turbulence [1, 2, 3]. Flux tube geometry is used, with local slab-like coordinates $(x, y, s)$ [4], corresponding roughly to the local radial, toroidal and parallel directions:

$$\frac{\partial \omega}{\partial t} + \{\phi, \omega\} = \mathcal{K}(n) + \nabla_{\shortparallel} J + \mu_\omega \nabla_\perp^2 \omega, \tag{1a}$$

$$\frac{\partial n}{\partial t} + \{\phi, n_{EQ} + n\} = \mathcal{K}(n - \phi) + \nabla_{\shortparallel}(J - u) + \mu_n \nabla_\perp^2 n, \tag{1b}$$

$$\frac{\partial}{\partial t}\left(\widehat{\beta} A_{\shortparallel} + \widehat{\mu} J\right) + \widehat{\mu}\{\phi, J\} = \nabla_{\shortparallel}(n_{EQ} + n - \phi) - CJ, \tag{1c}$$

$$\widehat{\varepsilon}\left(\frac{\partial u}{\partial t} + \{\phi, u\}\right) = -\nabla_{\shortparallel}(n_{EQ} + n). \tag{1d}$$

Parallel derivatives carry non-linearities entering through $A_{\shortparallel}$. $\mathcal{K}$ represents effects of curvature with $\omega_B = 2\frac{L_\perp}{R}$, R being the tokamak major radius and $L_\perp$ the mean gradient length:

$$\nabla_{\shortparallel} n = \frac{\partial n}{\partial s} - \widehat{\beta}\{A_{\shortparallel}, n\}, \qquad \mathcal{K}(n) = -\omega_B\left(\sin s \frac{\partial n}{\partial x} + \cos s \frac{\partial n}{\partial y}\right).$$

The parallel current $J$ is connected to the magnetic potential by $J = -\nabla_\perp^2 A_{\shortparallel}$. The electron parallel dynamics is controlled by the parameters

$$\widehat{\beta} = \frac{2\mu_0 p_{e,0}}{B^2}\widehat{\varepsilon}, \qquad \widehat{\mu} = \frac{m_e}{M_i}\widehat{\varepsilon}, \qquad C = 0.51\frac{L_\perp}{\tau_e c_s}\widehat{\mu} = \nu\widehat{\mu}, \tag{2}$$

with $\tau_e$ being the electron collision time. $n_{EQ}$ is an equilibrium density associated with neoclassical fields and currents. $\mathcal{K}(n_{EQ}) = -\nabla_{\shortparallel} J_{PS}$, which in turn is driven by the corresponding neoclassical potential $J_{PS} = \frac{1}{C}(\phi_{PS})$. The contribution of impurities to the gross plasma density $n_{i,0}$ is assumed to be negligible, i. e. $n_i = n_{i,0} + n_{imp} \approx n_{i,0}$. For cold impurities the ion-drift velocity is given by the $E \times B$- and the polarisation drift:

$$d_t n_{imp} = \frac{M}{Z\widehat{\varepsilon}}\nabla_\perp \cdot (n_{imp} d_t \nabla_\perp \phi) - n_{imp}\mathcal{K}(\phi) - \nabla_\parallel(n_{imp} u) - \mu_{imp}\nabla_\perp^2 n_{imp} \tag{3}$$

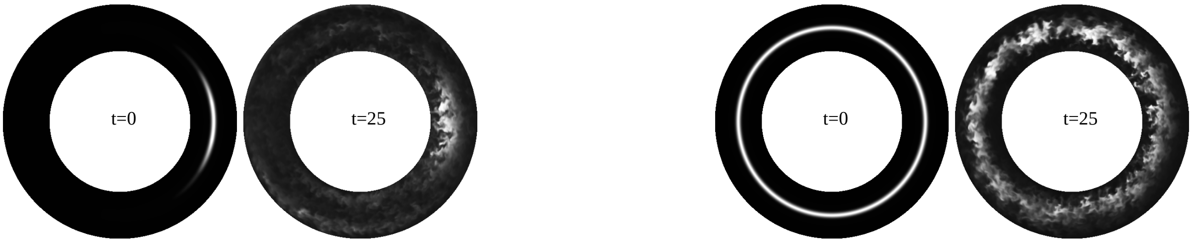


Figure 1: Impurity distribution projected onto a poloidal cross-section (radial dimension not to scale) initial distribution and after 25 time units corresponding to about 100$\mu$s.

We introduced the relative mass of the impurities $M = M_{imp}/M_i$ and $Z$ indicates their charge state. $d_t$ includes advection with the compressible $E \times B$ velocity. Finite inertia effects of the impurity ions enter through the ion-polarisation drift, however, in this paper we consider massless impurities.

Parameters were $\hat{\mu} = 5$, $q = 3$, magnetic shear $\hat{s} = 1$, $\omega_B = 0.05$, $\mu_\omega = \mu_n = 0.025$, corresponding to typical edge parameters. Simulations were performed on a grid with $128 \times 512 \times 32$ points and dimensions $64 \times 256 \times 2\pi$ in $x, y, s$ corresponding to an approximate dimensional size of 2.5 cm $\times$ 10 cm$\times$ 30 m [1]. Results are from a low $\hat{\beta} = 0.1$ run with $\nu = 2.295$. The initial impurity density $n_{imp}$ is a radially localized Gaussian on an impurity background. The diffusive term in Eq. (3) was chosen as $\mu_{imp} = 5\mu_n$. A prominent feature of the impurity behavior is the weak parallel convective transport, as parallel convection of impurities is due to the fluctuating parallel ion speed $u$ which is small ($u \approx 0.01$) compared to radial velocities of order one. This is clearly observed in Fig. 1. No significant parallel flow of the impurity density is observed, while significant radial mixing occurs. Parallel compressional effects are visible and arrange for finite passive density gradients at the high field side. An inward pinch effect is clearly observed at the outboard midplane. Starting from an initial impurity distribution homogeneous along $s$, this pinching velocity is seen to shift the impurity density towards the torus axis (Figure 1). The flux $\Gamma$ of the impurity ion species can be expressed by a diffusion coefficient $D$ and a velocity $V$, which is associated to a pinch effect:

$$\Gamma_y(s) = -D(s)\partial_x < n >_y + V(s) < n >_y \ . \qquad (4)$$

Profiles $< \cdot >_y$ are achieved by averaging over $y$. From scatter plots of $\Gamma(r)/ < n >_y$ versus

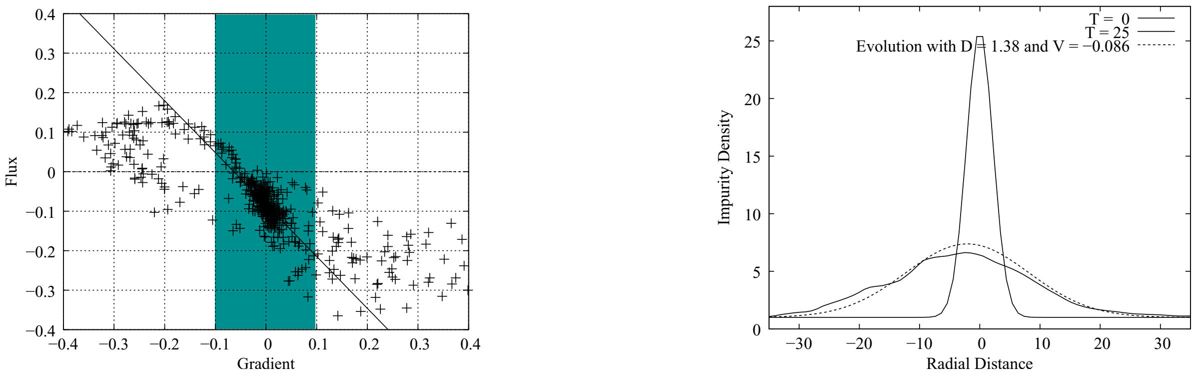


Figure 2: Left: Scatter plot (at high field side) of flux versus gradient with linear fit, gray area indicates gradients admissed for the fitting procedure. Rigth: Impurity density profile compared evolution of a Gaussian with $D$ and $V$ obtained by fitting.

$\partial_x < \ln n >_y$, values for $D(s)$ and $V(s)$ are obtained.

The poloidal (coordinate $s$) dependence of $D$ and $V$ is shown, with errors as obtained from the fitting routine, in Fig. 3. The effective convective velocity $V(s)$ changes sign and is at the high field side directed outwards. This can be consistently explained in the framework of Turbulent EquiPartition (TEP) [5, 6]: In the absence of parallel convection, finite mass effects and diffusion, Eq. (3) has the approximate Lagrangian invariant

$$L(s) = \ln n_{imp} + \omega_B cos(s)x - \omega_B sin(s)y \, . \tag{5}$$

TEP assumes the spatial homogenization of $L$ by the turbulence. This leads to profiles $< L(s) >_y = const(s)$. The strength of the "pinch" effect is proportional to the mixing properties of the turbulence and scales with the measured turbulent diffusion. Considering a stationary case with zero flux and combining Eq. (5) and Eq. (4) we obtain the following expression for the connection between pinch and diffusion:

$$V(s) = -\omega_B \cos(s) D(s) \, . \tag{6}$$

Averaged over a flux surface and assuming poloidally constant impurity density, a net impurity inflow results. This net pinch is proportional to the diffusion coefficient $D$ in agreement with experimental observations [7]. The proportionality constant will, however, depend on the amount of ballooning of the transport, which has been investigated f.x. in [1, 2, 3]. The level

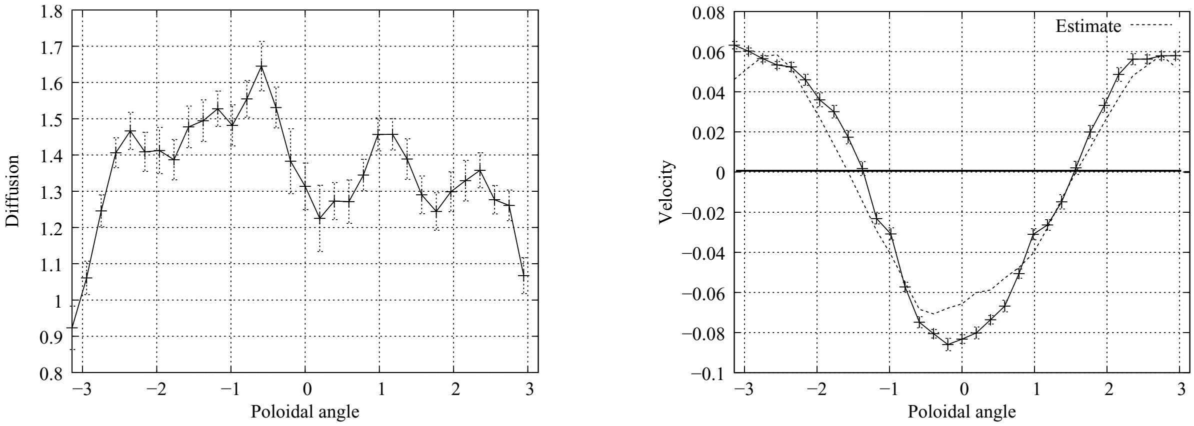


Figure 3: Impurity diffusion $D$ (top) and pinch velocity $V$ (bottom) over poloidal position ($s$) with error-bars. The pinch velocity is compared to $\omega_b * \cos(s) * D(s)$.

of ballooning of the transport increases with the transition from the drift regime to the MHD regime, as $\hat{\beta}$ increases to large values. Here, for small $hat\beta$ the ballooning of the transport is weak at about 70%.

Translated to dimensional values for typical large tokamak edge parameters we obtain $D(s) \propto 1.5 - 2.0\ \mathrm{m}^2/\mathrm{s}$ and $V(s) \propto (+60) - \ (-80)\ \mathrm{m/s}$ and a flux-surface averaged inward convection velocity of $< V >= -0.4\ \mathrm{m/s}$. Locally at the outboard midplane values of $V(s = 0)/D(s = 0) \sim -40\mathrm{m}^{-1}$ are found, again in agreement with experimental values [8].

This work was supported by the Danish Center for Scientific Computing through grants no. CPU-1101-08 and CPU-1002-17. Discussions with K.D. Zastrow and X. Garbet during a stay of VN at JET are gratefully acknowledged.

## References

[1] B. D. Scott, Plasma Phys. Control. Fusion **39**, 471 (1997).
[2] B. D. Scott, Plasma Phys. Control. Fusion **39**, 1635 (1997).
[3] V. Naulin, Phys. Plasmas **10**, 4016 (2003).
[4] B. D. Scott, Phys. Plasmas **8**, 447 (2001).
[5] J. Nycander and V. V. Yan'kov, Phys. Plasmas **2**, 2874 (1995).
[6] V. Naulin, J. Nycander, and J. Juul Rasmussen, Phys. Rev. Lett. **81**, 4148 (1998).
[7] M. E. Perry *et al.*, Nucl. Fusion **31**, 1859 (1991).
[8] R. Dux, Fusion Science and Technology **44**, 708 (2003).